

Magneto-optical response of Dynes superconductors

M. Šindler¹, F. Herman², F. Kadlec¹ and C. Kadlec¹

¹ Institute of Physics, Czech Academy of Sciences, Na Slovance 2, 182 21
Prague 8, Czech Republic

² Department of Experimental Physics, Comenius University, Mlynská
Dolina F2, 842 48 Bratislava, Slovakia

E-mail: sindler@fzu.cz

Abstract.

We investigate the terahertz conductivity of conventional superconductors in Voigt and Faraday magneto-optical configurations. In the Voigt geometry, an ultrathin superconducting film is fully penetrated by the magnetic field which interacts with the spin, thus modifying the magnitudes of the optical gap and of the density of the condensate. We provide an alternative interpretation of the recent experiments showing the gapless conductivity of a Nb film measured by Lee *et al.* [1] which describes better their data for magnetic field above 1 T. In the Faraday geometry, we analyze the terahertz conductivity of three NbN films with varying thicknesses using the Maxwell-Garnett model, treating vortices as normal-state inclusions within a superconducting matrix. Moreover, we effectively account for ubiquitous pair-conserving and magnetic-field-dependent pair-breaking disorder scattering processes using the model of Herman and Hlubina [2].

1. Introduction

Magnetic field has dramatic effects on superconductivity—it induces screening currents and the appearance of a vortex lattice (orbital effect), and it interacts with the electron spin (Zeeman effect). The contributions of these two effects to the optical conductivity depend on the orientation of the applied magnetic field with respect to the sample. In the Faraday geometry, the magnetic field is applied perpendicular to the surface, which results in screening currents suppressing the field inside the superconductors, thus the orbital effect usually dominates. In the Voigt geometry, the magnetic field is directed along the surface. In films with a thickness smaller than the penetration depth, the magnetic field is only weakly suppressed inside the film and the Zeeman effect dominates.

Abrikosov developed a theoretical approach able to account for the pair-breaking effect of paramagnetic impurities [3]. Later, Maki [4] showed that the Abrikosov approach could be used for other pair-breaking agents including external magnetic field. Finally, Skalski, Betdeder-Matibet and Weiss [5] worked out an integral expression for optical conductivity which accounts for pair-breaking effects. Their SBW model was recently used to explain THz spectra of niobium, NbN and Nb_{0.5}Ti_{0.5}N films in the Voigt geometry [1, 6, 7]. Xi *et al.* [6, 7] observed the suppression of the pair-correlation gap Δ and of the spectroscopic gap Ω_G in ultrathin films of NbN and Nb_{0.5}Ti_{0.5}N in agreement with the SBW model [5], using the pair-breaking parameter α to account for the effects of the magnetic field. While for NbN, α is linearly proportional to B ($\alpha \sim B$), for Nb_{0.5}Ti_{0.5}N, a square law has been observed ($\alpha \sim B^2$).

In similar measurements on an ultrathin niobium film [1], Lee *et al.* managed to fully suppress the spectroscopic gap at 2.4 T for a temperature of 1.5 K. In the interval 2.4–3.5 T, $\Omega_G = 0$ but Δ still persists. For magnetic fields above 3.5 T, the superconductivity is lost. Their THz spectra are well described by the SBW model even in the gapless regime. However, in contrast to the observed data, the SBW model predicts a steep fall in the real part of conductivity near low frequencies for magnetic fields of 1–2 T. Moreover, in both mentioned cases [1, 6], the resulting interpretation of the SBW model is questionable, since it uses orbital effect-originated relation between pair-breaking parameter and the second power of the amplitude of the external magnetic field [8] while in Voigt geometry setup the Zeeman splitting effect usually dominates.

In this paper, we propose a way of interpreting the THz spectra in the magnetic field by replacing the SBW model effectively with the one developed by Herman and Hlubina (HH model) [2] including the heuristic dependence of the pair-breaking parameter

on the external magnetic field, in a similar fashion as in Ref. [9]. Notice that the HH model has basically the same number of parameters as the SBW model. This makes them equally computationally challenging and allows for a simple comparison of their results.

In the Faraday geometry, there are two approaches to describing the terahertz conductivity. In the first one, vortex cores are treated as normal-state inclusions inside a superconducting environment and this inhomogeneous system can be described as a homogeneous one with an effective complex conductivity. Maxwell-Garnett theory [10] is the most often used [11, 12] as it correctly captures the topology of isolated vortex cores. In this approach, vortices are static and possible vortex motion and related consequences are thus neglected. In the second approach, the two-fluid model is utilized in various theoretical models [13, 14, 15, 16] to describe the vortex dynamics as the dominant contribution to both the real and the imaginary parts of conductivity. The inherent weakness of the two-fluid model is that it does not account for the presence of the superconducting gap in the spectra, which can be justified for frequencies well below the gap but fails in the vicinity of gap and for even higher frequencies. In this article, we propose possible improvements of Xi's approach [11], where the complex conductivity of the superconducting matrix is not described by its zero-field value but the HH model is used to account for the presence of the pair-conserving and pair-breaking scattering processes, the latter assumed to increase in the presence of the external magnetic field.

2. Theory

In this section, we shortly introduce the fundamental aspects of the SBW and the HH models.

First, the density of states (DOS) needs to be examined. The BCS theory [17] postulates the oversimplified formula for the DOS

$$\text{DOS} = \Re \left(\frac{u}{\sqrt{u^2 - 1}} \right), \quad (1)$$

where \Re stands for the real part of the complex value and the parameter $u = E/\Delta$ equals the energy normalized to the value of the gap where $E=0$ at Fermi level. For energy within the interval $-\Delta < E < \Delta$ there are no states and the DOS diverges at $E = \pm\Delta$. The Zeeman effect leads to a shift in the DOS for up and down spins, thus their respective DOS are $2\mu_B B$ apart, where B is the magnetic field and $\mu_B = 9.274 \times 10^{-24} \text{ J T}^{-1}$ denotes the Bohr magneton. However, the spin-orbit scattering leads to mixing the states for spin up and down states. The spin-orbit scattering rate is proportional to the fourth power of the atomic number [18, 19], thus the described shift

can be clearly observed only in samples with atoms with a low atomic number such as Al films [20]. Here, we study the response of Nb and NbN films in the magnetic field, thus the DOS for up and down spins are smeared into one broad peak. Further details can be found in the Fulde's review paper [21].

In the limit of large spin-orbit scattering, the SBW model generalizes the DOS from the BCS theory, Eq. (1), and u is evaluated from the following nonlinear equation:

$$u\Delta = E + \alpha \frac{u}{\sqrt{u^2 - 1}} \quad (2)$$

where α is the Maki's pair-breaking parameter. Eq. (2) has an analytical solution [22] corresponding to the root of the quartic function. The pair-correlation gap Δ is both temperature and magnetic field-dependent. In zero magnetic field, its value corresponds to the gap value obtained from the optical measurements Ω_G . However, with increasing magnetic field, or more generally with increasing α , $\Omega_G(B)$ decreases faster than $\Delta(B)$. At a critical value of the magnetic field, the superconductor enters a so-called gapless state where Ω_G becomes zero while $\Delta > 0$ thus allowing the persistence of the superconducting state. At even higher values of the magnetic field, Δ becomes zero and the superconductivity is finally fully suppressed.

On the other hand, the Dynes formula [23] accounts for the broadening of the DOS by phenomenologically introducing the broadening parameter Γ :

$$\text{DOS} = \Re \left(\frac{E + i\Gamma}{\sqrt{(E + i\Gamma)^2 - \Delta^2}} \right). \quad (3)$$

The microscopic origin of the Dynes formula was unclear for a long time, but in a recent paper [24], it was shown that the formula given by Eq. (3) is valid in systems with a pair-breaking, magnetic, classical disorder provided that the pair-breaking scattering probability distribution has a Lorentzian distribution with width Γ within the Coherent Potential Approximation (CPA). In the presented context, the parameter Γ accounts for the influence of the magnetic (spin-flip) scattering. In this way we model the influence of Zeeman splitting and spin-orbit interaction for Voigt and the presence of the screening currents in Faraday geometries in a simple phenomenological way. We will also assume that the effective pair-breaking parameter $\Gamma(B)$ is an increasing function of the external magnetic field, playing thus similar role as α in the SBW model. Moreover, the solution of the CPA equations [24] results in the convenient form of the superconducting gap function $\Delta(E)$ and the wavefunction renormalization $Z(E)$ [2]

$$\Delta(E) = \bar{\Delta} \left/ \left(1 + \frac{i\Gamma}{E} \right) \right.,$$

$$Z(E) = \left(1 + \frac{i\Gamma}{E} \right) \left(1 + \frac{i\Gamma_s}{\Omega(E)} \right),$$

where \dagger $\Omega(E) = \sqrt{(E + i\Gamma)^2 - \bar{\Delta}^2}$ and $\bar{\Delta} = \bar{\Delta}(T)$ corresponds to the temperature dependent gap [25]. This formulation introduces the pair-breaking Γ and the pair-conserving Γ_s scattering rates. It results in the Dynes tunnelling density of states and fulfils the Anderson theorem [26]. Although the main advantage of the HH model from our perspective is the clear identification of the pair-conserving and pair-breaking scatterings in the superconducting state, it also results in a natural normal state limit $\Delta(E) = 0$ and $Z_N(E) = (1 + i\Gamma_N/E)$, where $\Gamma_N = \Gamma_s + \Gamma$ unifies the effect of the disorder, as expected. In the normal state, the overall scattering rate is related to the scattering time τ in the Drude model for optical conductivity by $\Gamma_N = \hbar/(2\tau)$.

2.1. Optical conductivity utilizing HH model

The optical conductivity of Dynes superconductors is calculated from the integral expression resulting from the Green function approach [2, 24, 27]. Furthermore, its numerical evaluation is as costly as that which makes use of the generalized Mattis-Bardeen formula [28] but, unlike the latter, it allows also for pair-breaking processes.

When discussing the optical response of Dynes superconductor, it is customary to follow Nam [29] and introduce three complex functions: the density of states $n(\omega)$, the density of pairs $p(\omega)$ and a function $\epsilon(\omega)$ with dimension of energy

$$n(\omega) = n_1 + in_2 = \frac{\omega}{\sqrt{\omega^2 - \Delta^2(\omega)}} = \frac{\omega + i\Gamma}{\Omega(\omega)}, \quad (4)$$

$$p(\omega) = p_1 + ip_2 = \frac{\Delta(\omega)}{\sqrt{\omega^2 - \Delta^2(\omega)}} = \frac{\bar{\Delta}}{\Omega(\omega)}, \quad (5)$$

$$\epsilon(\omega) = \epsilon_1 + i\epsilon_2 = Z(\omega)\sqrt{\omega^2 - \Delta^2(\omega)} = \Omega(\omega) + i\Gamma_s \quad (6)$$

The functions $n(\omega)$ and $p(\omega)$ are obviously linked together, and they satisfy the constraint $n^2(\omega) - p^2(\omega) = 1$. Note that the functions $n_1(\omega)$, $p_2(\omega)$ and $\epsilon_2(\omega)$ are even, whereas the functions $n_2(\omega)$, $p_1(\omega)$ and $\epsilon_1(\omega)$ are odd in ω .

Next, let us introduce auxiliary variables

$$H_1(x, y) = \frac{1 + n(x)n^*(y) + p(x)p^*(y)}{2[\epsilon^*(y) - \epsilon(x)]},$$

$$H_2(x, y) = \frac{1 - n(x)n(y) - p(x)p(y)}{2[\epsilon(y) + \epsilon(x)]}. \quad (7)$$

Assuming the local limit of the electromagnetic field response, motivated by the characteristic values of the considered mean free paths $\ell \sim 1\text{nm}$, the resulting

\dagger We choose the square root branch so that the signs of $\text{Re}\{\Omega(E)\}$ and E are the same.

optical conductivity can be written as [2, 27]

$$\sigma_s(\omega) = \frac{iD_0}{\omega} \int_{-\infty}^{\infty} d\omega' \left[(f(\omega' + \omega) - f(\omega')) H_1(\omega' + \omega, \omega') - f(\omega') (H_2(\omega' + \omega, \omega') + H_2^*(\omega', \omega' - \omega)) \right], \quad (8)$$

where $D_0 = ne^2/m$ is the normal-state Drude weight and we utilized the Fermi-Dirac distribution $f(E) = 1/(1 + e^{E/(k_B T)})$. Notice also, that eq. 8 is formulated using units $\hbar = 1$. As shown in $T = 0$ K limit, the spectroscopically gapless state is present for arbitrary $\Gamma > 0$ [30].

3. Results

3.1. Voigt geometry

In the Voigt geometry, the in-plane external magnetic field fully penetrates ultrathin superconducting films allowing us to study the effects of a homogeneous magnetic field on their superconducting properties. Here, we partly revisit the work of Lee *et al.* [1]. The authors measured the complex conductivity of a $d = 58$ nm thick Nb film with a critical temperature of $T_c = 8$ K, see Fig 1. From the imaginary part of the conductivity, the London penetration depth λ_L was estimated as $0.1 \mu\text{m}$, thus the film was thin compared to its penetration depth, i.e. $\lambda_L \gg d$. The magnetic field averaged over the film thickness d can be approximated as $H_{avg} \approx H_0(1 - d^2/(12\lambda_L^2))$ which confirms, for the given parameters, a very homogeneous internal magnetic field. Physically, such a Nb film is too thin to develop a sufficiently thick layer of screening currents able to screen the magnetic field.

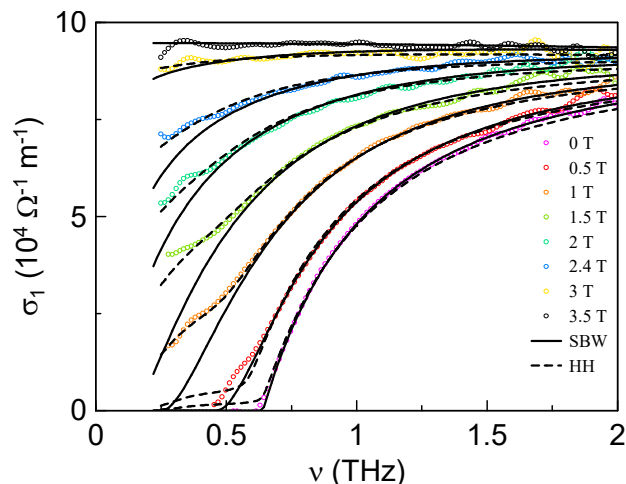


Figure 1. Real part of complex conductivity $\sigma_1(\nu)$ of a 58 nm thick Nb film in Voigt geometry measured by Lee *et al.* [1]. Experimental data (points) are theoretically described by the SBW model (solid lines) and the HH model (dashed lines). The imaginary part $\sigma_2(\nu)$ is not shown here.

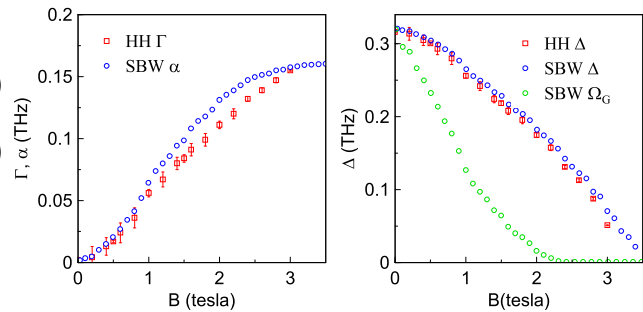


Figure 2. Magnetic field dependence of Γ and α (left) and Δ and Ω_G (right) determined from fits of the experimental data by Lee *et al.* [1]. Circles: SBW model, squares: HH model.

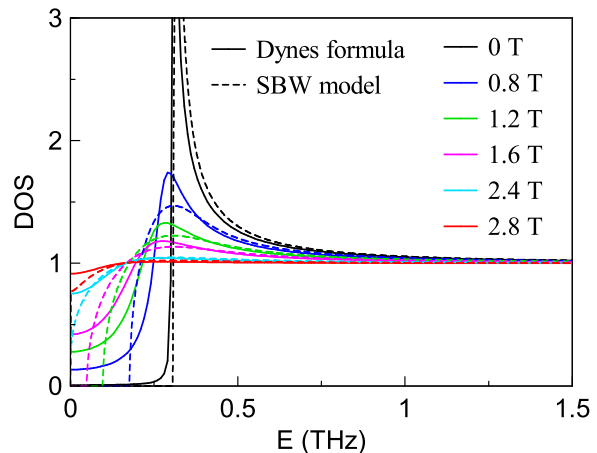


Figure 3. Density of states (DOS) in the vicinity of the Fermi energy normalized to the DOS in the normal state for magnetic fields up to 2.8 T. The DOS of the HH and the SBW models are slightly different even for $B=0$ due to the slight difference in the zero field fits. The DOS was calculated with the Dynes formula, Eq. 3, using parameters from the fit by the HH model (solid lines), and with the SBW model using parameters from the fit of the THz data (dashed lines).

First, the SBW model was used to fit the zero-field experimental data using the zero-field gap Δ_0 , the DC conductivity σ_0 and the pair-breaking parameter α as free parameters. In the magnetic field, $\alpha(B)$ is the only free parameter of the fit since other variables are not field-dependent. The field dependences of the pair-correlation gap $\Delta(B)$ and of the spectroscopic gap $\Omega_G(B)$ were determined from the values of $\alpha(B)$ within the SBW model [5]. Measurements up to 3.6 T revealed the suppression of the pair-correlation gap $\Delta(B)$ and of the spectroscopic gap $\Omega_G(B)$. Above 2.4 T, $\Omega_G = 0$ but $\Delta(B) \neq 0$ and the superconductor enters a gapless state until the superconductivity is completely suppressed at 3.5 T. The SBW model correctly predicts a shift in Ω_G with the applied magnetic field, but it fails to describe the shape of the real part of the THz conductivity $\sigma_1(\omega)$ in detail, see solid lines in Fig 1.

We decided to compare the results of the SBW

model with the theoretical prediction of Herman and Hlubina [2]. First, we fitted the experimental data in zero magnetic field with the DC conductivity σ_0 , the zero-field gap $\Delta_{\Gamma \rightarrow 0}$, the pair-conserving scattering rate Γ_s and the pair-breaking scattering rate Γ as free parameters. The value of the gap Δ is approximated by the formula [24, 25]

$$\Delta = \sqrt{\Delta_{\Gamma \rightarrow 0}[\Delta_{\Gamma \rightarrow 0} - 2\Gamma]}, \quad (9)$$

which is valid in the limit of zero temperature. For non-zero magnetic fields, we used the resulting values except for the pair-breaking scattering rate $\Gamma(B)$ which was treated as a free parameter. The magnetic field dependence of gap $\Delta(B)$ is governed by $\Gamma(B)$ using equation 9. The conductivity $\sigma(\nu)$ predicted by the HH model, see dashed lines in Fig 1, decreases more slowly at low frequencies. For low magnetic fields, the SBW model seems to be more accurate, but from 1 T, the HH model describes more precisely the experimental results. In Fig. 2, we compare the values of the parameters of the SBW and of the HH theoretical models. The pair-correlation gap Δ and Γ , respectively α , have qualitatively and quantitatively the same dependence on the magnetic field. To better understand the difference between these models, we plot the density of states within the SBW model and compare it to the Dynes formula justified by the HH model. The parameters for the DOS are taken from the fits of the complex conductivity $\sigma(\nu)$ with each model. They are qualitatively different. While the SBW DOS has no states for $|E| < \Omega_G$ for $B < 2.4$ T, the Dynes formula fills the gap gradually, see Fig 3.

3.2. Faraday geometry

We measured the optical response of three NbN films of different thicknesses (5.3, 11.5, and 30.1 nm) using time-domain THz spectroscopy. The experimental setup, as well as the treatment used to extract the THz conductivity spectra from our data, are reported in detail in [9].

In the Faraday geometry, the magnetic field and consequently the vortices are perpendicular to the plane of the film. Their presence substantially alters the zero-field properties in type II superconductors. To interpret the experimental results, we use a model in which the vortices are approximated as normal-state cylinders surrounded by a superconducting matrix. The spectral response of the superconducting matrix is provided by the HH model [2] where Γ changes with the magnetic field and describes the pair-breaking effect of the field. The gap is modified due to Γ according to the equation 9.

In the THz range, the conditions for the so-called long-wavelength limit are fulfilled: the wavelengths are much longer than the distances between the vortices,

Table 1. Parameters of NbN films: d_f film thickness, T_c critical temperature, Γ_s field independent value of pair-conserving scattering rate, $\Delta_{\Gamma \rightarrow 0}$ value of the gap corresponding to $\Gamma \rightarrow 0$ and σ_0 DC conductivity

Sample	d_f nm	T_c K	Γ_s THz	$\Delta_{\Gamma \rightarrow 0}$ THz	σ_0 $\mu\Omega^{-1}\text{m}^{-1}$
NbN@MgO	5.3	13.9	5.9	0.62	1.55
NbN@Si	11.5	12	5.4	0.51	0.45
NbN@MgO	30.1	15.5	4.4	0.65	2.52

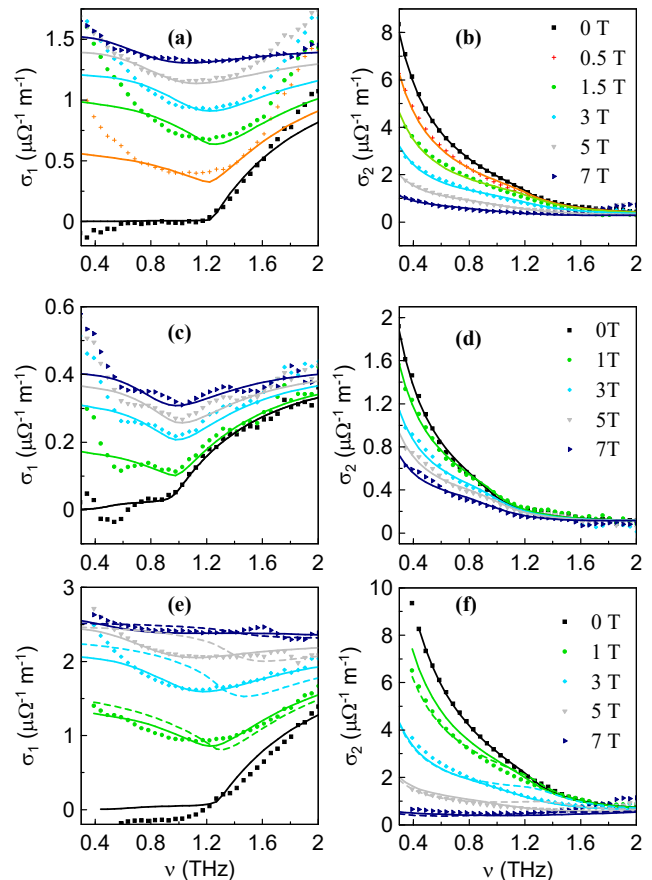


Figure 4. Real (a, c, e) and imaginary (b, d, f) parts of the THz conductivity of NbN thin films measured in the Faraday geometry at 2 K up to 7 T. Three NbN samples of different thicknesses were studied: (a-b) $d_f = 5.3$ nm, (c-d) $d_f = 11.5$ nm and (e-f) $d_f = 30.1$ nm. Symbols: experimental data, lines: fits using the Maxwell-Garnett theory and the HH model.

thus the inhomogeneous system can be represented by an effective optical conductivity. The geometry of the normal state inclusions inside the superconducting matrix can be well described by the Maxwell-Garnett model [10] which yields the effective conductivity $\tilde{\sigma}_{\text{MG}}$:

$$\frac{\tilde{\sigma}_{\text{MG}} - \tilde{\sigma}_s}{\tilde{\sigma}_{\text{MG}} + K\tilde{\sigma}_s} = f_n \frac{\tilde{\sigma}_n - \tilde{\sigma}_s}{\tilde{\sigma}_n + K\tilde{\sigma}_s}, \quad (10)$$

where f_n and $\tilde{\sigma}_n$ are the volume fraction and the conductivity of the normal state vortex cores, respectively; further, $\tilde{\sigma}_s$ the conductivity of the

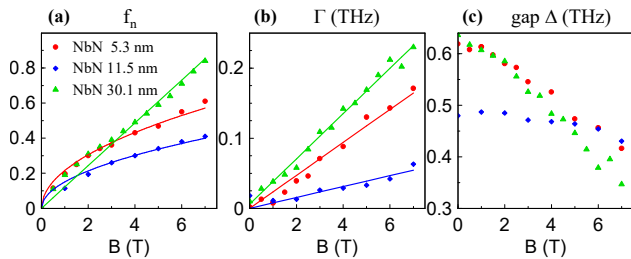


Figure 5. The normal state volume fraction f_n , the pair-breaking rate Γ and the superconducting gap Δ as functions of the magnetic field. Points: values obtained by the fits of the spectra with the HH model, lines: fitted curves.

superconducting matrix. K is the shape factor of inclusions and has been taken as $K = 1$ which corresponds to the value for cylinders with their axis perpendicular to the electric field.

The THz conductivity spectra of the three NbN films are shown in Fig. 4. In our fits, we used two free parameters: the volume fraction of the vortex cores f_n , and the pair-breaking scattering rate Γ which influences the shape of the superconducting conductivity spectra $\sigma_s(\nu)$. The remaining parameters are taken from the zero field fit and they are field independent. In Fig. 4 (e) and (f), we show illustrative examples of fits using the zero-field $\sigma_s(\nu)$ (dashed curves) in order to demonstrate the importance of $\Gamma(B)$.

The pair-breaking scattering rate Γ is proportional to the magnetic field for all 3 studied NbN films, see Fig. 5(b). The gap Δ (Fig. 5(c)) was evaluated using equation 9 from the fitted values of Γ .

The normal fraction should be a linear function of the magnetic field ($f_n = B/B_{c2}$), but this holds only for the thickest sample, see Fig. 5(a). The square root dependence $f_n \propto aB^{1/2}$ observed by Xi *et al.* [11] successfully describes $f_n(B)$ for the 5 nm and the 11.5 nm thick NbN films. A similar square root dependence was also observed in overdoped $\text{La}_{2-x}\text{Ce}_x\text{CuO}_4$ [31].

The sublinear behaviour can be attributed to the limitations of the simple effective medium model or possibly due to the shrinking of the vortex cores [32, 33] with increasing magnetic field. Finally, the upturn in the real part of the conductivity $\sigma_1(\omega)$ at low frequencies which is not fully described by our model results from the vortex dynamics [12], since this effect can not taken into account in the effective medium approaches.

4. Conclusions

The theoretical model by Herman and Hlubina [2] for Dynes superconductors allows us to calculate the optical conductivity for varying ratios of the pair-conserving and pair-breaking processes. We have

demonstrated that the HH model can well describe the optical conductivity in magnetic fields both in Voigt and Faraday geometries by varying the pair-breaking scattering rate Γ . In this way, the model serves as an effective phenomenology describing the pair-breaking effect of the increasing external magnetic field suppressing the T_c , filling the gap in the density of states, and affecting the optical conductivity. In the Voigt geometry, the HH model offers a better theoretical description of the optical conductivity of the Nb thin film measured by Lee *et al.* [1] than the SBW model used earlier. In the Faraday geometry, the THz response of the vortex lattice is described by the Maxwell-Garnett effective medium theory [10] with the properties of the superconducting matrix following the HH model [2]. As the range of the found parameters $\Gamma \lesssim \Delta \lesssim \Gamma_s/10$ fulfills the natural expectations and suggests possible usage of the HH model in the dirty limit [2], the presented formulation allows for the explicit presence of the pair-conserving scattering. This may be useful in the analysis of cleaner systems.

Last but not least, let us emphasize that the presented analysis utilizes the HH model as an effective phenomenology with the fewest free parameters, taking into account $\Gamma(B)$ as the effective pair-breaking scattering rate. This approach allows for straightforward comparison with the related results reported in the current literature. The difference in shapes of $\Gamma(B)$ dependence considering different geometries originates probably from the combination of the Zeeman splitting and spin-orbit interaction in Voigt and from the orbital effects in the Faraday geometry. To proceed further with the analysis of the presented experiments and distinguish the role of individual effects on terahertz conductivity measurements in more detail, one would need a more elaborate description of the Zeeman splitting and of the spin-orbit interaction, to take into account the screening current generation (orbital effects), as well as the role of intrinsic pair-breaking and pair-conserving disorder. In the best-case scenario, the model could go beyond the Born approximation limit, allowing for higher magnitudes of the individual effects.

Acknowledgements

We are grateful to K. Ilin and M. Siegel for preparing and characterizing the NbN sample, as well as to Jae Hoon Kim and Ji Eun Lee, who were very kind to provide their data [1]. We also acknowledge the financial support by the Czech Science Foundation (Project No. 21-11089S), by European Union and the Czech Ministry of Education, Youth and Sports (Project TERAFIT - CZ.02.01.01/00/22 008/0004594) and by the INTER-COST (Project LUC24098). This

work was also supported by the Slovak Research and Development Agency under the Contract no. APVV-23-0515 and by the European Union's Horizon 2020 research and innovation programme under the Marie Skłodowska-Curie Grant Agreement No. 945478.

References

- [1] Lee J E, Choi J, Jung T S, Kim J H, Choi Y J, Sim K I, Jo Y and Kim J H 2023 *Nature Communications* **14** 2737
- [2] Herman F and Hlubina R 2017 *Phys. Rev. B* **96**(1) 014509
- [3] Abrikosov A and Gor'kov L 1961 *Soviet Phys. JETP* **12** 1243
- [4] Maki K 1963 *Progress of Theoretical Physics* **29** 603–605 ISSN 0033-068X
- [5] Skalski S, Betbeder-Matibet O and Weiss P R 1964 *Phys. Rev.* **136**(6A) A1500–A1518
- [6] Xi X, Hwang J, Martin C, Tanner D B and Carr G L 2010 *Phys. Rev. Lett.* **105**(25) 257006
- [7] Xi X 2011 *Conventional and time-resolved spectroscopy of magnetic properties of superconducting thin films* dissertation thesis University of Florida
- [8] Parks R 1969 *SUPERCONDUCTIVITY* vol 2 (Marcel Dekker, INC., New York) chap 18, pp 1071 – 1073
- [9] Šindler M, Kadlec F and Kadlec C 2022 *Phys. Rev. B* **105**(1) 014506
- [10] Garnett J C M and Larmor J 1904 *Philos. Trans. Royal Soc. of London. Ser. A* **203** 385–420
- [11] Xi X, Park J H, Graf D, Carr G L and Tanner D B 2013 *Phys. Rev. B* **87**(18) 184503
- [12] Šindler M, Tesař R, Koláček J, Szabó P, Samuely P, Hašková V, Kadlec C, Kadlec F and Kužel P 2014 *Supercond. Sci. Technol.* **27** 055009
- [13] Coffey M W and Clem J R 1991 *Phys. Rev. Lett.* **67**(3) 386–389
- [14] Brandt E H 1991 *Phys. Rev. Lett.* **67**(16) 2219–2222
- [15] Dulčić A and Požek M 1993 *Physica C: Superconductivity* **218** 449–456 ISSN 0921-4534
- [16] Lipavský P, Elmurodov A, Lin P J, Matlock P and Berdiyrov G R 2012 *Phys. Rev. B* **86**(14) 144516
- [17] Bardeen J, Cooper L N and Schrieffer J R 1957 *Phys. Rev.* **106**(1) 162–164
- [18] Crow J E, Strongin M and Bhatnagar A K 1974 *Phys. Rev. B* **9** 135–138
- [19] Meservey R and Tedrow P 1976 *Physics Letters A* **58** 131–132 ISSN 0375-9601
- [20] Meservey R, Tedrow P M and Fulde P 1970 *Phys. Rev. Lett.* **25**(18) 1270–1272
- [21] Fulde P 1973 *Advances in Physics* **22** 667–719
- [22] Assig M, Etzkorn M, Enders A, Stiepany W, Ast C R and Kern K 2013 *Review of Scientific Instruments* **84** 033903 ISSN 0034-6748
- [23] Dynes R C, Narayanamurti V and Garno J P 1978 *Phys. Rev. Lett.* **41**(21) 1509–1512
- [24] Herman F and Hlubina R 2016 *Phys. Rev. B* **94**(14) 144508
- [25] Lebedeva A and Herman F 2025 *J. Supercond. Nov. Magn.* **38**
- [26] Anderson P W 1959 *J. Phys. Chem. Solids* **11**
- [27] Lebedeva A, Hladký M, Polák M and Herman F 2024 (*Preprint* 2409.04203) URL <https://arxiv.org/abs/2409.04203>
- [28] Zimmermann W, Brandt E, Bauer M, Seider E and Genzel L 1991 *Physica C* **183** 99–104 ISSN 0921-4534
- [29] Nam S B 1959 *Phys. Rev.* **156** 470
- [30] Herman F and Hlubina R 2021 *Phys. Rev. B* **104**
- [31] Tagay Z, Mahmood F, Legros A, Sarkar T, Greene R L and Armitage N P 2021 *Phys. Rev. B* **104**(6) 064501
- [32] Sonier J E 2004 *Journal of Physics: Condensed Matter* **16** S4499
- [33] Ning Y X, Song C L, Wang Y L, Chen X, Jia J F, Xue Q K and Ma X C 2010 *Journal of Physics: Condensed Matter* **22** 065701